Dalton Transactions

Heteropolynuclear $PdAg_4$ Complexes with Self-Assembled Trans-Chelating $\{(Ar_2pz)_3Ag_2\}$ Units

Journal:	*Dalton Transactions*
Manuscript ID	DT-COM-05-2025-001078.R1
Article Type:	Communication
Date Submitted by the Author:	17-May-2025

Complete List of Authors:	Kinoshita, Kana; Nagasaki University Yang, Yiming; Nagasaki University Nagano, Shiho; Nagasaki University Horiuchi, Shinnosuke; The University of Tokyo, Graduate School of Arts and Sciences Nakao, Yoshihide; Kyushu Sangyo University, Applied Chemistry and Biochemistry Omoto, Kenichiro; Graduate School of Science and Technology Nara Institute of Science and Technology, Sakuda, Eri; Nagasaki University, Division of Chemistry and Materials Science Arikawa, Yasuhiro; Nagasaki University, Graduate School of Engineering Umakoshi, Keisuke; Nagasaki University, Division of Chemistry and Materials Science

COMMUNICATION

Heteropolynuclear $PdAg_4$ Complexes with Self-Assembled Trans-Chelating $\{(Ar_2pz)_3Ag_2\}$ Units

Received 00th January 20xx,
Accepted 00th January 20xx

DOI: 10.1039/x0xx00000x

Kana Kinoshita,[a] Yiming Yang,[a] Shiho Nagano, [a] Shinnosuke Horiuchi, *[a,b] Yoshihide Nakao, [c] Kenichiro Omoto, [a] Eri Sakuda, [a] Yasuhiro Arikawa [a] and Keisuke Umakoshi *[a]

Herein, we report novel square-planar Pd(II) complexes bearing two $Ag_2(Ar_2pz)_3$ units as self-assembled trans-chelating ligands. This structural motif is unique to Pd(II) ions and cannot be obtained from a Pt(II) metal source owing to the stronger dative bonding nature of the Pt(II) ion compared to that of the Pd(II) ion.

Utilization of the coordination mode of neutral pyrazole (R_2pzH) and anionic pyrazolato (R_2pz) ligands, where R denotes alkyl or aryl group, have been developed over several decades, because they can act as bridging ligands to hold two metal ions in close proximity, enabling to induce specific metal–metal interaction.[1] For example, pyrazolato ligands can bind coinage metal ions (Au(I), Ag(I), and Cu(I)) to form triangular M_3 complexes with strong metallophilic interaction.[2–8] Similarly, butterfly-shaped dinuclear Pt(II) complexes having bridged pyrazolato ligands have been studied widely, owing to a drastic emission color change derived from Pt···Pt distance tunable by the steric bulkiness of the substituent groups on the pyrazolato ligands.[9]

Pyrazole ligands can also bind two different metal ions to afford heteropolynuclear metal complexes with significant heterometallic metal–metal interactions.[1,9] In addition to the interesting structural motifs of coordination complexes based on pyrazole and pyrazolato ligands, the close proximity of different metal ions combines their molecular orbitals around the metal ions to give rise to new physical properties from the mixed-metal complexes, which are not observable in each component. We have developed synthetic procedures and luminescent studies of highly emissive heteropolynuclear Pt(II)–Ag(I) complexes containing pyrazolato (R_2pz) bridging ligands.[10] In particular, the square-planar Pt(II) complex units involving pyrazolato ligands can produce brightly luminescent sandwich-type heteropolynuclear complexes $[Pt_2M_4(Me_2pz)_4]$ (M = Ag(I), Cu(I); Me_2pz = 3,5-dimethylpyrazolate) and $[Pt_2Au_2M_2(Me_2pz)_4]$ (M = Ag(I), Cu(I)). The photo luminescence originated from the excited state mainly composed of in-phase combination of molecular orbitals of metal ions with fine-tuning of the emission color by incorporating coinage metal ions.[11,12] The basicity of the bridging pyrazolato ligand effectively controls the stoichiometry between the Pt(II) ion and pyrazolato ligand to alter the photophysical properties.[13] Furthermore, the steric bulkiness of the pyrazolato ligands also modulated the structure and rigidity of the precious metal sandwich complexes, enabling reversible encapsulation of Ag ion within the Pt–Ag cluster cores via the formation of multiple Pt→Ag dative bonds.[14–18]

In contrast to the rich photochemistry of Pt(II) complexes, emissive Pd(II) complexes are still limited, although Pd(II) ions produce square-planar coordination complexes similar to Pt(II) complexes. This is mainly because the d-d excited states of Pd(II) complexes lie at a lower energy level than the emissive excited state and readily show thermal deactivation, which causes effective quenching of the luminescence from the complex.[19,20] Thus, luminescent Pd(II) complexes have been developed by increasing the energy of the d-d excited states of Pd(II) ions and decreasing those of the intra-ligand (^{3}IL) and ligand-to-ligand charge transfer (^{3}LLCT) excited states using suitable multidentate cyclometalated ligands.[21–27] In addition, understanding the intermetallic interactions between Pd(II) ions and coinage metal ions has also attracted much attention because they play a central role in cooperative catalysis.[28–30] Thus, we evaluated the structures and photophysical properties of heteropolynuclear complexes based on square-planar Pd(II) complexes and Ag(I) ions bridged by pyrazolato ligands.

Herein, we report the synthesis, structure, and photophysical properties of Pd–Ag heteropolynuclear complexes bearing 3,5-diphenylpyrazolato (Ph_2pz) ligands and

[a] *Division of Chemistry and Materials Science, Graduate School of Engineering, Nagasaki University, 1-14 Bunkyo-machi, Nagasaki, 852-8521 (Japan).*
[b] *Department of Basic Science, Graduate School of Arts and Sciences, The University of Tokyo, 3-8-1 Komaba, Meguro-ku, Tokyo 153-8902 (Japan).*
[c] *Department of Life Science, Faculty of Life Science, Kyushu Sangyo University, 2-3-1 Matsukadai, Higashi-ku, Fukuoka 813-8503 (Japan).*
E-mail: shoriuchi@g.ecc.u-tokyo.ac.jp, kumks@nagasaki-u.ac.jp

Electronic Supplementary Information (ESI) available: Synthetic procedures, characterization, X-ray structures, theoretical studies of the complexes. See DOI: 10.1039/x0xx00000x

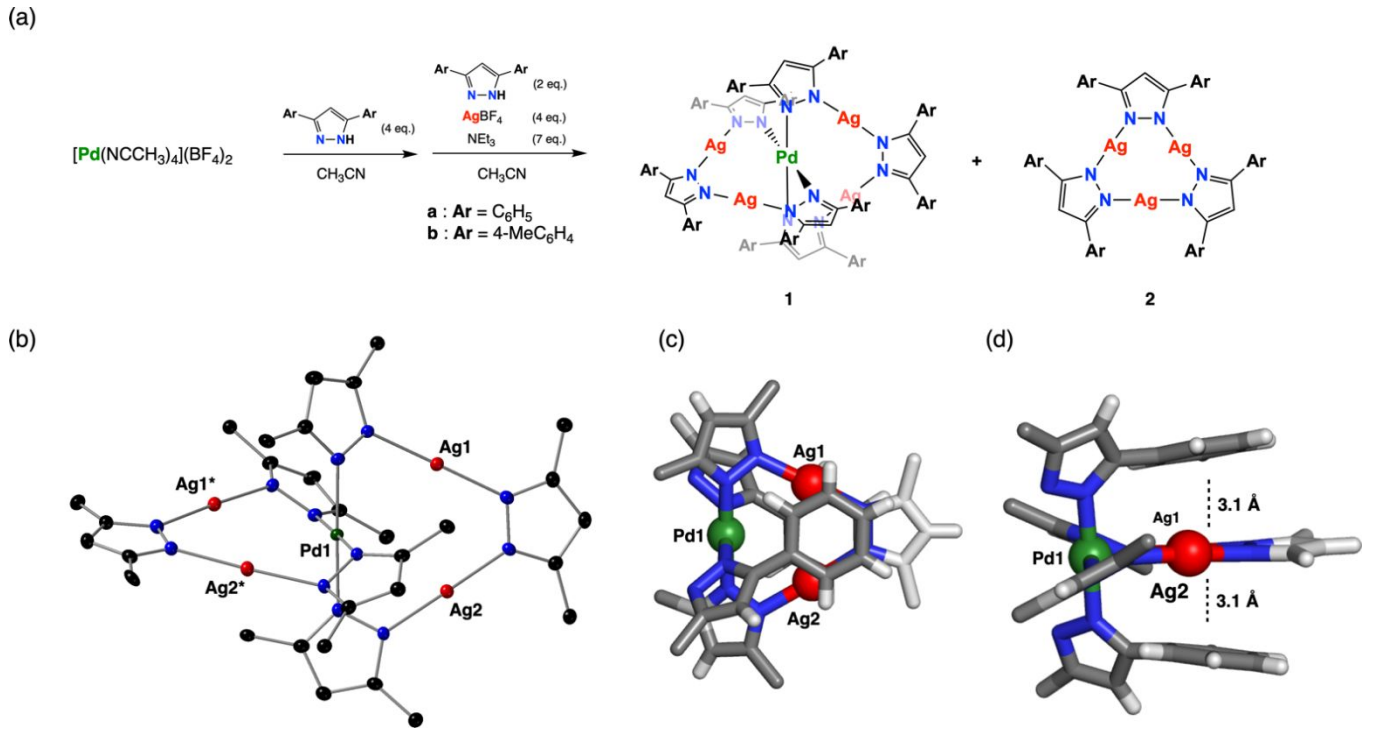

Fig. 1 (a) Schematic representation of the synthesis of $PdAg_4$ complex **1** and Ag_3 complex **2**. (b) ORTEP drawings (50% probability ellipsoids) of the $PdAg_4$ complex **1a**. The phenyl groups on the pyrazolato ligands were omitted for clarity. (c, d) Relative orientations between the $PdAg_2$ plane and phenyl substituents on the pyrazolato ligands: (c) view perpendicular to the $PdAg_2$ plane and (d) side view of the $PdAg_2$ plane. This X-ray structure clearly shows that the $PdAg_2$ cores were sandwiched between two phenyl moieties of the Ph_2pz ligands via π–π and Ag–π interactions (< 3.3 Å). Hydrogen atoms and solvent molecules are omitted for clarity. Selected atomic distances (Å) for **1a**: Pd1···Ag1, 3.3865(6); Pd1···Ag2, 3.3611(6); Ag1···Ag2, 3.3789(7).

their derivatives. The Pd(II) ion has a square-planar geometry supported by two unique self-assembled trans-chelating $\{(Ar_2pz)_3Ag_2\}$ moieties (Ar = C_6H_5, 4-$(CH_3)C_6H_4$), which have never been obtained in Pt(II) complex systems. Intramolecular π-π stacking between the aromatic substituents on the pyrazolato ligands and the strong π-acidic Ag_2 core contributed to the formation of unique cluster structures, as confirmed by single-crystal X-ray structural analysis. To the best of our knowledge, the $\{(Ar_2pz)_3Ag_2\}$ moieties are the first example of trans-spanning chelate ligands formed by self-assembly because trans-spanning ligands are often constructed using ethynyl and pyridyl or aryl groups.[31–39] The $PdAg_4$ complexes exhibited bright photoluminescence in the solid states at 77 K. These features of the Pd-based cluster significantly differed from those of Pt(II)-based cluster preferring sandwich structure, which probably reflect weak electron-donating character of Pd metal.[40,41]

According to the synthetic procedure for Pt–Ag complexes with Ph_2pz ligands, we initially attempted to check the reaction of Pd(II) salt with Ph_2pzH and Ag salts.[13] As a result, we found that the $PdAg_4$ complex **1a** was unexpectedly obtained as the main product by the reaction of $[Pd(NCCH_3)_4](BF_4)_2$ complex salt with 3,5-diphenylpyrazole (Ph_2pzH), $AgBF_4$, and NEt_3 in a net one-pot, two-step reaction (Fig. 1a). After the reaction, the ^1H NMR spectrum of the unpurified product indicated the formation of **1a** and triangular Ag_3 complex **2a** (Fig. S13†). The $PdAg_4$ complex **1a** is less soluble in CH_2Cl_2, enabling the separation of the mixture by crystallization from a CH_2Cl_2/*n*-pentane solution to afford fine crystals of **1a** (28% isolated yield based on $[Pd(CH_3CN)_4](BF_4)_2$).

The molecular structure of **1a** was undoubtedly confirmed by single-crystal X-ray structural analysis (Fig. 1b). The X-ray structure of **1a** clearly showed that the Pd(II) ion possessed a square-planar geometry and triangular $\{(Ph_2pz)_3Ag_2\}$ units bound to the Pd(II) metal center as an eight-membered trans-chelating ligand, whose structure was significantly different from that of a sandwich-shaped Pt_2Ag_4 heteropolynuclear complex containing Ph_2pz ligands.[13] The $PdAg_4$ complex contained an S_4 improper rotation center at the Pd(II) ion, and the $\{(Ph_2pz)_3Ag_2\}$ units consisted of two chemically inequivalent pyrazolato ligands in a 2:1 ratio, which was in good agreement with the observation of the ^1H NMR spectrum of **1a** (Fig. S1†). These results strongly suggest that the unique $PdAg_4$ structure is maintained in the solution state. Notably, the dihedral angle between the two $PdAg_2$ planes defined by each of the three metal atoms, Pd1, Ag1, and Ag2 and Pd1, Ag1*, and Ag2*, was not perpendicular (90°) but 54.7°, suggesting that the $PdAg_4$ complex was largely distorted in the solid state owing to the packing effect (Fig. S17 and S18†). This structural flexibility reflects the labile nature of the Pd–N and Ag–N coordination bonds and intramolecular (π-π and Ag–π) interactions discussed below.

The $PdAg_4$ structure appears to be formed when the Ag(I) ions in the two triangular Ag_3 complexes are replaced one by

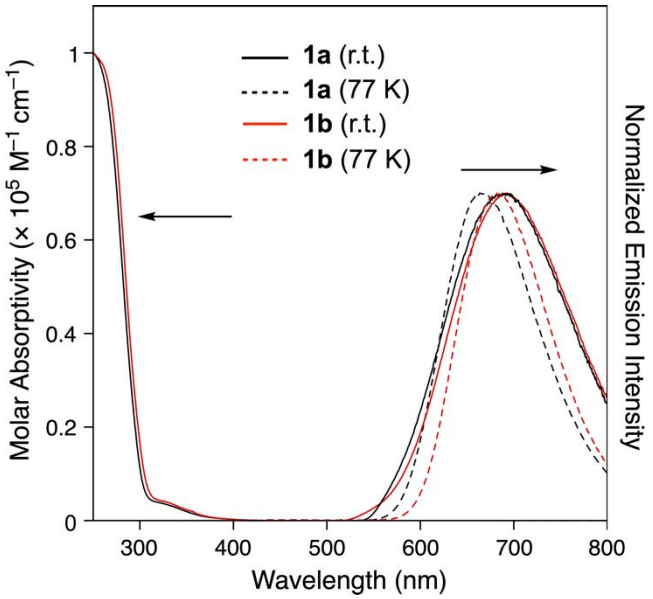

Fig. 2 UV-Vis absorption (CH_2Cl_2, r.t.) and normalized emission spectra of the $PdAg_4$ complexes **1** in the solid state (λ_{ex} = 350 nm).

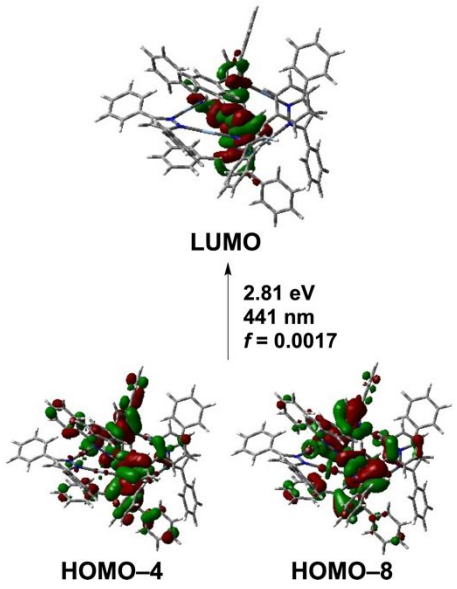

Fig. 3 Molecular orbitals of $PdAg_4$ complex **1a** in the gas phase, displayed by the TD-DFT calculations.

one by the same Pd(II) ion. Thus, we attempted an alternative approach to synthesizing $PdAg_4$ complex **1a** through a transmetalation reaction of $[Pd(NCCH_3)_4](BF_4)_2$ with Ag_3 complex **2a**. However, the ^{1}H NMR spectrum of the reaction mixture revealed that $PdAg_4$ complex **1a** was not formed by this reaction (Fig. S14†). This result indicates that the Pd-pyrazole adduct formed in the first step is an important intermediate in the formation of $PdAg_4$ structure. Notably, the $PtAg_4$ complex analog was not obtained via a similar intermediate, Pt-pyrazole adduct.[13] It is known that Pt(II) ion can strongly bind acidic coinage metal ion, such as Ag(I) ion, to form Pt→M dative bond, which is supported by the higher basicity of Pt(II) ion than that of Pd(II) ion.[42] Owing to the stronger basicity of central metal ion, the Pt(II) complex system is likely to give sandwich-type Pt_2Ag_4 heteropolynuclear complexes, effectively stabilized by orbital overlapping between 6p and 5p orbitals of two Pt(II) and four Ag(I) ions, respectively.[11,13]

The isolated $PdAg_4$ complex did not decompose to form the Ag_3 complex, even in the solution state, over several days. Therefore, the $PdAg_4$ structure is thermodynamically stable. To understand the high thermodynamic stability of the $PdAg_4$ framework, we carefully examined the crystal structure of **1a**. The pyrazolato–Ag–pyrazolato–Ag–pyrazolato plains were sandwiched between two phenyl substituents of the pyrazolate ligands in the other $PdAg_2$ triangular unit (Fig. 1c and 1d). Thus, the trans-chelating $(Ph_2pz)_3Ag_2$ units were effectively stabilized by intramolecular π-stacking between the π-acidic dinuclear $Ag_2(pz)$ moiety and electron-rich phenyl groups in the pyrazolato ligands.[43,44] The 3,5-di(4-methylphenyl)pyrazole ligand also gave the corresponding $PdAg_4$ complex **1b** in a similar reaction procedure as **1a**, as confirmed by NMR studies in solution (Fig. S7–S11†) and X-ray structural analysis of the crystalline state of the $PdAg_4$ complex (Fig. S19–S21†). In contrast, a Pd-pyrazole adduct using 3,5-dimethylpyrazole (Me_2pz) afforded a sandwich-shaped Pd_2Ag_4 complex, $[Pd_2Ag_4(Me_2pz)_8]$, rather than this $PdAg_4$ structure.[45] Thus, the phenyl moieties on the pyrazolato ligand played a crucial role in forming the $PdAg_4$ structure, which was effectively stabilized by intramolecular π-π and Ag-π interactions (Fig. 1c and 1d).

The X-ray structures of the $PdAg_4$ complexes, **1a** and **1b**, clearly showed short contacts among the metal ions in the cluster units, implying Pd···Ag and Ag···Ag interactions. As sandwich-shaped Pt_2Ag_4 complexes exhibit tunable photoluminescence behavior owing to the in-phase

Table 1 Spectroscopic and photophysical data of the complexes in the crystalline states.

Complex	Temp. (K)	λ_{em} (nm)	Φ_{em} (%)	τ [a] (μs)	τ_{ave} [b] (μs)	$k_r \times 10^3$ [b] (s^{-1})	$k_{nr} \times 10^4$ [b] (s^{-1})
1a	r.t.	689	8	τ_1 = 5.6 (A_1 = 0.81), τ_2 = 11.6 (A_2 = 0.19)	7.6	10.6	12.2
	77	664	64	τ_1 = 75 (A_1 = 0.53), τ_2 = 248 (A_2 = 0.47)	200	3.1	0.18
1b	r.t.	693	6	τ_1 = 10.8 (A_1 = 0.48), τ_2 = 22.9 (A_2 = 0.52)	19.2	3.12	4.89
	77	680	59	τ_1 = 44 (A_1 = 0.87), τ_2 = 238 (A_2 = 0.13)	131	4.51	0.31

[a] Emission decay curve was analysed by the equation ($I(t) = I_0(A_1\exp(t/\tau_1) + A_2\exp(t/\tau_2))$) using the nonlinear least-squares method. [b] Calculated by the equations $\Phi_{em} = k_r / (k_r + k_{nr}) = k_r\tau_{ave}$ and $\tau_{ave} = (A_1\tau_1^2 + A_2\tau_2^2)/(A_1\tau_1 + A_2\tau_2)$.

combination of the p orbitals of the metal ions,[11,12] their photoluminescence properties can be easily varied by the extent of heterometallic metal–metal interactions. Thus, we studied the photoluminescence properties of the $PdAg_4$ complexes (Fig. 2 and Table 1). The emission spectra of the crystalline sample of **1** at room temperature showed broad emission spectra (**1a**: λ_{max} = 689 nm, Φ = 8%; **1b**: λ_{max} = 693 nm, Φ = 6%). The observed emission lifetimes of **1** were in the microsecond regime (τ_{ave} = 7.6 μs (**1a**), 19.2 μs (**1b**)), indicating that the emission stemmed from the triplet state (phosphorescence). Despite the negligible emission of the crystalline sample of Ag_3 complex **2a** at room temperature, the red emission of **1** with moderate intensity implies the contribution of Pd(II) ions in the emissive state of these $PdAg_4$ complexes, although **1** is non-emissive in the solution state, as is often observed for Pd(II) complexes.[18,19] Notably, the emission properties were significantly enhanced at 77 K owing to the effective inhibition of the thermal nonradiative decay of the complexes in the photo-excited process (Table 1). The broad emission spectra of **1** showed a blue shift (**1a**: λ_{max} = 664 nm, Φ = 64%; **1b**: λ_{max} = 680 nm, Φ = 59%), and a structured emission spectrum (λ = 419, 446, 470 nm, Φ = 8%) was observed for **2a** at 77 K (Fig. S15†).

To shed light on the absorption spectra of **1**, the absorption bands of these complexes were theoretically investigated using the time-dependent density functional theory (TD-DFT) method. The TD-DFT calculations revealed that the lowest energy absorption band was mainly assigned to the combination of d-d*(Pd), ligand-to-metal charge-transfer (LMCT) [π(Ph_2pz) → d(Pd)], and ligand-centered (LC) transitions (Fig. 3). In contrast, the emissive state was mainly attributed to the metal-centered (^{3}MC(d-d*)) excited states by the DFT calculations based on the optimized triplet excited-state structure (Fig. S23†). The assignment of the emissive state is consistent with the moderate ligand-field strength of the $Pd(Ar_2pz)_4$ moiety and the experimental results. However, the possibility of the contribution of another excited state, such as ^{3}LMCT, to the emissive state cannot be excluded because of the packing effect and intermolecular interactions in the solid state. These characteristics of **1a** were different from those of Pt–Ag cluster complexes bearing pyrazolato bridging ligands.[9]

Conclusions

We elucidated the structures and photophysical properties of square-planar Pd(II) complexes bearing two $Ag_2(Ar_2pz)_3$ units as self-assembled trans-spanning chelating ligands. Although Pd(II) and Pt(II) ions possess the same coordination geometry (square-planar) and very similar ionic radii, the structure of the cluster core constructed by Ph_2pz ligands for the Pd–Ag system is different from that for the Pt–Ag system. This might be owing to the lower basicity of Pd(II) ion than Pt(II) ion, and the Pd–Ag cluster structure is predominantly stabilized by intramolecular π-π and Ag-π interactions rather than the heterometallic interactions. Photophysical and theoretical studies of Pd–Ag clusters supported negligible orbital overlap between the Pd(II) and Ag(I) metal centers. The dative bonding character between elements has been discussed for several decades. This study demonstrated that the balance between intramolecular (π-π and metal-π) interactions and the strength of the dative bond is key to controlling the structure of heteropolynuclear cluster complexes. It also provides a better understanding of the dative bonding nature between metallic elements and unique structural motifs with chemical and physical properties originating from the incorporated elements.

Data availability

The data supporting this article have been included as part of the ESI. Crystallographic data have been deposited at the Cambridge Crystallographic Data Centre (CCDC) under deposition numbers 2431540–2431541 for **1a** and **1b**, and can be obtained from https://www.ccdc.cam.ac.uk/structures/.

Conflicts of interest

There are no conflicts to declare

Acknowledgements

This work was financially supported by JSPS KAKENHI Grant Numbers JP19H04587, JP20K05542, JP20H05834, JP22H04554, JP23K04775, JP23H0394, JST SPRING Grant Number JPMJSP2172, the Izumi Science and Technology Foundation, precious metals research grants from Tanaka Kikinzoku Memorial Foundation, and the Nagasaki University WISE programme. This work was conducted using research equipment shared in the MEXT project for promoting public utilization of advanced research infrastructure (Program for supporting introduction of the new sharing system) Grant Number JPMXS0422500320. We are grateful to J. Nagaoka for X-ray measurements.

Notes and references

1 M. A. Halcrow, *Dalton Trans*., 2009, 2059–2073.
2 K. Fujisawa, Y. Ishikawa, Y. Miyashita and K. Okamoto, *Inorg. Chim. Acta.,* 2010, **363**, 2977–2989.
3 Y. Morishima, D. J. Young and K. Fujisawa, *Dalton Trans.*, 2014, **43**, 15915–15928.
4 H. V. R. Dias, C. S. P. Gamage, J. Keltner, H. V. K. Diyabalanage, I. Omari, Y. Eyobo, N. R. Dias, N. Roehr, L. McKinney, and T. Poth, *Inorg. Chem*., 2007, **46**, 2979–2987.
5 H. V. R. Dias, S. Singh, and C. F. Campana, *Inorg. Chem*., 2008, **47**, 3943–3945.
6 M. A. Omary, O. Elbjeirami, C. S. P. Gamage, K. M. Sherman, and H. V. R. Dias, *Inorg. Chem*., 2009, **48**, 1784–1786.
7 J. S. Lakhi, M. R. Patterson, and H. V. R. Dias, *New. J. Chem*., 2020, **44**, 14814–14822.
8 J. Zheng, Z. Lu, K. Wu, G.-H. Ning and D. Li, *Chem. Rev*., 2020, **43**, 9675–9642.
9 S. Horiuchi and K. Umakoshi, *Coord. Chem. Rev*., 2023, **476**, 214924.
10 S. Horiuchi and K. Umakoshi, *Chem. Rec.* 2021, **21**, 469–479.
11 K. Umakoshi, T. Kojima, K. Saito, S. Akatsu, M. Onishi, S. Ishizaka, N. Kitamura, Y. Nakao, S. Sakaki and Y. Ozawa, *Inorg, Chem*., 2008, **47**, 5033–5035.

12 K. Umakoshi, K. Saito, Y. Arikawa, M. Onishi, S. Ishizaka, N. Kitamura, Y. Nakao and S. Sakaki, *Chem. Eur. J.,* 2009, **15**, 4238–4242.
13 S. Akatsu, Y. Kanematsu, T. Kurihara, S. Sueyoshi, Y. Arikawa, M. Onishi, S. Ishizaka, N. Kitamura, Y. Nakao, S. Sakaki and K. Umakoshi, *Inorg. Chem*., 2012, **51**, 7977–7992.
14 M. Ueda, S. Horiuchi, E. Sakuda, Y. Nakao, Y. Arikawa and K. Umakoshi, *Chem. Commun.*, 2017, **53**, 6405–6408.
15 S. Horiuchi, S. Moon, A. Ito, J. Tessarolo, E. Sakuda, Y. Arikawa, G. H. Clever and K. Umakoshi, *Angew. Chem. Int. Ed*., 2021, **60**, 10654–10660.
16 S. Horiuchi, Y. Yang, M. Ueda, E. Sakuda, Y. Arikawa and K. Umakoshi, *Eur. J. Inorg. Chem.*, 2022, **2022**, e202200497.
17 Y. Yang, S. Horiuchi, K. Omoto, E. Sakuda, Y. Arikawa and K. Umakoshi, *Chem. Lett.*, 2024, **53**, upad004.
18 Y. Yang, S. Horiuchi, K. Omoto, E. Sakuda, Y. Arikawa and K. Umakoshi, *Chem. Eur. J.*, 2025, accepted article, DOI:10.1002/chem.202500948.
19 L. Bischoff, C. Baudequin, C. Hoarau and E. P. Urriolabeitia, *Adv. Organomet. Chem*. 2018, **69**, 73–134.
20 D. Dalmau and E. P. Urriolabeitia, *Molecules*, 2023, **28**, 2663.
21 P. K. Chow, C. Ma, W.-P. To, G. S. M. Tong, S.-L. Lai, S. C. F. Kui, W.-M. Kwok and C.-M. Che, *Angew. Chem. Int. Ed*., 2013, **52**, 11775–11779.
22 C. Zou, J. Lin, S. Suo, M. Xie, X. Chang and W. Lu, *Chem. Commun*., 2018, **54**, 5319–5322.
23 J. Lin, C. Zou, X. Zhang, Q. Gao, S. Suo, Q. Zhuo, X. Chang, M. Xie and W. Lu, *Dalton Trans*., 2019, **48**, 10417–10421.
24 G. Li, J. Zheng, X. Fang, K. Xu, Y.-F. Yang, J. Wu, L. Cao, J. Liu and Y. She, *Organometallics*, 2021, **40**, 472–481.
25 Y. She, K. Xu, X. Fang, Y.-F. Yang, W. Lou, Q. Zhang and G. Li, *Inorg. Chem*., 2021, **60**, 12972–12983.
26 J. Lin, M. Xie, X. Zhang, Q. Gao, X. Chang, C. Zou and W. Lu, *Chem. Commun*., 2021, **57**, 1627–1630.
27 I. Maisuls, C. Wang, M. E. G. Suburu, S. Wilde, C.-G. Daniliuc, D. Brünink, N. L. Doltsinis, S. Ostendorp, G. Wilde, J. Kösters, U. Resch-Genger and C. A. Strassert, *Chem. Sci*, 2021, **12**, 3270–3281.
28 M. H. Pérez-Temprano, J. A. Casares and P. Espinet, *Chem. Eur. J*., 2012, **18**, 1864–1884.
29 Á. L. Mudarra, S. Martínez de Salinas and M. H. Pérez-Temprano, *Org. Biomol. Chem*., 2019, **17**, 1655–1667.
30 U. B. Kim, D. J. Jung, H. J. Jeon, K. Rathwell and S. Lee, *Chem. Rev*., 2020, **120**, 13382–13433.
31 J. E. Fiscus, S. Shotwell, R. C. Layland, M. D. Smith, H.-C. zur Loye and U. H. F. Bunz, *Chem. Commun*., 2001, 2674–2675.
32 H. G. Vang, Z. L. Driscoll, E. R. Robinson, C. E. Green, E. Bosch and N. P. Bowling, *Eur. J. Org. Chem.*, 2016, 891–895.
33 T. Kawano, J. Kuwana, T. Shinomaru, C.-X. Du and I. Ueda, *Chem. Lett.*, 2001, **30**, 1230–1231.
34 E. Bosch and C. L. Barnes, *Inorg. Chem.*, 2001, **40**, 3097–3100.
35 E. Bosch, C. L. Barnes, N. L. Brennan, G. L. Eakins and B. E. Breyfogle, *J. Org. Chem.*, 2008, **73**, 3931–3934.
36 S. Shotwell, H. L. Ricks, J. G. M. Morton, M. Laskoski, J. Fiscus, M. D. Smith, K. D. Shimizu, H.-C. zur Loye and U. H. F. Bunz, *J. Organomet. Chem.*, 2003, **671**, 43–51.
37 Y.-Z. Hu, C. Chamchoumis, J. S. Grebowicz and R. P. Thummel, *Inorg. Chem.*, 2002, **41**, 2296–2300.
38 G. Meyer-Eppler, F. Topić, G. Schnakenburg, K. Rissanen and A. Lützen, *Eur. J. Inorg. Chem.*, 2014, 2495–2501.
39 T. R. Schulte, J. J. Holstein, L. Krause, R. Michel, D. Stalke, E. Sakuda, K. Umakoshi, G. Longhi, S. Abbate, G. H. Clever, *J. Am. Chem. Soc.*, 2017, **139**, 6863–6866.
40 M. Sircoglou, S. Bontemps, G. Bouhadir, N. Saffon, K. Miqueu, W. Gu, M. Mercy, C.-H. Chen, B. M. Foxman, L. Maron, O. V. Ozerov and D. Bourissou, *J. Am. Chem. Soc.*, 2008, **130**, 16729–16738.
41 E. D. Litle and F. P. Gabbaï, *Angew. Chem. Int. Ed*., 2022, **61**, e202201841.
42 D. Campillo, D. Escudero, M. Baya and A. Martín, *Chem. Eur. J*. 2022, **28**, e202104538.
43 H. V. R. Dias and C. S. P. Gamage, *Angew. Chem. Int. Ed*., 2007, **46**, 2192–2194.
44 S. M. Tekarli, T. R. Cundari and M. A. Omary, *J. Am. Chem. Soc*., 2008, **130**, 1669–1675.
45 G. A. Ardizzoia, G. L. Monica, S. Cenini, M. Moret and N. Masciocchi, *J. Chem. Soc. Dalton Trans*., 1996, 1351–1357.

Data availability

The data supporting this article have been included as part of the ESI. Crystallographic data have been deposited at the Cambridge Crystallographic Data Centre (CCDC) under deposition numbers 2431540–2431541 for 1a and 1b, and can be obtained from https://www.ccdc.cam.ac.uk/structures/